WEP Warwick Evans Publishing

International Journal of Global Economics and Management
ISSN: 3005-9690 (Print), ISSN: 3005-8090 (Online) | Volume 3, Number 1, Year 2024
DOI: https://doi.org/10.62051/ijgem.v3n1.57
Journal homepage: https://wepub.org/index.php/IJGEM/index

Carbon Emission Right Price Prediction based on IOWHA Operator Vector Angle Cosine Combination Deep Learning

Yu Liu *

School of Statistics and Applied Mathematics, Anhui University of Finance and Economics, Bengbu Anhui, China

*Corresponding Author: Yu Liu

ABSTRACT

The relentless exacerbation of the greenhouse effect poses a significant challenge to the progress and sustainability of human civilization. Carbon emission rights serve as a pivotal gauge of the carbon trading market's dynamics. Examining the impact of carbon emission rights prices can shed light on how governments indirectly influence these prices through mechanisms such as carbon emission quotas and permits. This study focuses on analyzing the transaction prices of carbon emission rights quotas within the Guangzhou carbon trading market spanning from January 2015 to March 2023. Leveraging a selection of 17 variables across the realms of energy prices, macroeconomics, financial markets, and ecological environment, and drawing insights from the predictive outcomes of three distinct sub-models—namely Ridge Regression, Random Forest Regression, and Long Short-Term Memory neural network (LSTM)—a novel IOWHA operator vector angle cosine combination model is devised. The findings underscore that this combined model harnesses the predictive strengths of each sub-model, effectively curbing prediction discrepancies, and enhancing overall accuracy. The integration of these methodologies represents an optimal fusion for predictive modeling.

KEYWORDS

IOWHA operator; LSTM; Combined prediction; Carbon emission rights

1. INTRODUCTION

The phenomenon of the greenhouse effect poses a pervasive global challenge, with the surge in carbon emissions serving as the chief catalyst for its escalation. The intensive energy consumption accompanying our nation's developmental trajectory inevitably engenders profound environmental repercussions attributable to technological and resource-related factors. As per data from the World Bank, China eclipsed the United States in 2005 to claim the mantle of the world's foremost emitter of carbon, with its emissions surging to a monumental 10,523 million tons by 2021, representing a commanding 31.06% of global greenhouse gas emissions. In response to the daunting environmental exigencies and imperatives to combat climate change, China has proactively instituted various measures and enacted a suite of stringent environmental protection statutes. Noteworthy among these initiatives is China's unveiling of the "Dual Carbon Target" in September 2020, wherein it pledged to achieve a carbon peak by 2030 and attain carbon neutrality by 2060, underscoring its steadfast commitment to global sustainability and climate resilience.

The carbon trading market has gradually emerged as a pivotal policy instrument aimed at curbing carbon emissions via market mechanisms [16]. Within this framework, greenhouse gas emissions are conceptualized as tradable "commodities". Operating under governmental regulatory frameworks that constrain the aggregate volume of carbon emissions over defined timeframes, enterprises and affiliated entities engage in the exchange of allocated carbon emission quotas or permits within the market. Enhanced by advancements in emission reduction and energy-saving technologies within enterprises, surplus emission quotas can be effectively traded within the carbon market. This facilitates the mitigation of emissions by entities facing challenges in immediate emissions reduction due to elevated costs, thereby ensuring an efficient allocation of emission quotas within the predetermined total [17].

Initiating its endeavors in 2013, China embarked on the establishment of a pilot carbon emission trading system. By December 31, 2021, the cumulative trading volume within the seven pilot carbon markets had surged to 483 million tons, with transactions valuing at 8.622 billion yuan. This underscores the systematic and progressive evolution of the domestic carbon market within China.

Carbon emission rights represent the entitlement to utilize the limited environmental resource of the atmosphere. Functioning as a crucial metric within the carbon market landscape, the price of carbon emission rights serves as a pivotal indicator of market dynamics. Effective allocation of carbon emission rights and the advancement of a low-carbon economy hinge upon the establishment of a rational carbon trading price.

Exploration of the nuanced attributes of carbon emission rights constitutes a valuable avenue for comprehensive investigation into the determinants influencing carbon emission rights pricing. Such research endeavors are instrumental in facilitating the formulation of informed policies by governmental bodies, thereby fostering more efficacious measures to mitigate carbon emissions, bolster environmental preservation efforts, and steadily progress towards the objectives of carbon peak and carbon neutrality.

Domestic research on carbon emission prices focuses on the carbon price formation mechanism, factors affecting carbon price fluctuations, and trends and laws of carbon price fluctuations. The analysis of factors affecting carbon emission prices shows a development trend from single to diversified [11]. Based on the fact that fossil energy combustion is the main source of carbon emissions, Wei [14]. focused on the impact of the single factor of fossil energy price changes on China's carbon trading prices. In the study of multivariate factors affecting carbon emission prices, domestic and foreign scholars have made great contributions. After determining the multiple factors affecting carbon emission prices, most of the studies analyzed and ranked the weights of the variables of each influencing factor through different model methods, and obtained the factors with the greatest impact on carbon emission prices under the conditional background, and on this basis, gave explanations and suggestions of practical economic significance. Wang and Hu [2] used the FGLS method to find that oil prices and GDP have a greater impact on carbon prices; Guo[1] used the LASSO method to perform dimensionality reduction stepwise regression analysis on factors of different dimensions; Yi et al. [4] ranked the weights of various factors affecting carbon emission prices by establishing a MIV-BP neural network model for EU carbon emission prices. Zou and Wei [5], Wang and Lu [6] conducted in-depth research on the factors affecting carbon quota prices and CER spot prices based on the VEC model. Lu [13] established a VAR vector autoregression model and compared the weights of the variables of each influencing factor by variance decomposition. Lu [12] analyzed and compared the factors affecting carbon emission prices in the five pilot regions in China from the perspective of parameter sensitivity.

This paper endeavors to forecast the transaction price of carbon emission quotas within China's carbon emission market through the integration of deep learning techniques and composite prediction methodologies. By amalgamating deep learning approaches with conventional multivariate regression methods, it adopts a comprehensive strategy aimed at enhancing predictive accuracy. Leveraging the combined prediction mechanism of the IOWHA operator alongside cosine vector angle calculations, the study seeks to develop an optimized composite prediction model. This model is refined through the assignment of distinct weights to individual feature sub-models, thus facilitating a more robust and nuanced forecasting framework for carbon emission quota transaction prices.

2. COMBINED PREDICTION MODEL

2.1. Sub-model Construction Method

2.1.1. Ridge Regression

Ridge Regression is a kind of regression method, which belongs to statistical methods. It is also called weight decay in machine learning. Some people also call it Tikhonov regularization. There are two main problems that ridge regression solves: one is when the number of predictor variables exceeds the number of observed variables (predictor variables are equivalent to features, and observed variables are equivalent to labels), and the other is when there is multicollinearity between data sets, that is, there is a correlation between predictor variables. The (matrix) form of a regression analysis is as follows:

$$y = \sum_{j=1}^{p} \beta_j x_j + \beta_0 \tag{1}$$

The goal of using the least squares method to solve the above regression problem is to minimize the following formula:

$$\hat{\beta} = argmin_\beta \sum_{i=1}^{N} \left(y_i - \beta_0 - \sum_{j=1}^{p} \beta_j x_i\right)^2 \tag{2}$$

Ridge regression adds a penalty term to the above minimization objective:

$$\hat{\beta}^{bridge} = arg\ min_\beta \left\{\sum_{i=1}^{N} \left(y_i - \beta_0 - \sum_{j=1}^{p} \beta_j x_i\right)^2 + \lambda \sum_{j=1}^{p} {\beta_j}^2\right\} \tag{3}$$

2.1.2 Random Forest Regression

Random forest is a supervised machine learning method that is built by integrating decision trees as the base learner. It further introduces randomness into the training process of decision trees, making them have excellent anti-overfitting and anti-noise capabilities.

The steps of random forest regression are as follows:

A) Extract training sets from the original sample set. In each round, use the bootstrap sampling method to extract n training samples from the original sample set (sampling with replacement). Perform k rounds of extraction in total to obtain k training sets. (The k training sets are independent of each other)

B) Each time a training set is used to obtain a model, k training sets are used to obtain a total of k models.

C) Calculate the mean of the above model as the final regression result.

2.1.3 Long Short-Term Memory Neural Network

Recurrent Neural Network (RNN) is a type of neural network. RNN is very effective for data with sequence characteristics. It can mine the temporal information and semantic information in the data. Due to its internal structure, it has excellent performance and effect on short sequence tasks. However, when long sequences are associated, gradient calculation abnormalities will occur during backpropagation, causing gradient disappearance or explosion. Compared with RNN, Long Short-Term Memory Neural Network (LSTM) can effectively capture the semantic association between long sequences and alleviate the phenomenon of gradient explosion or disappearance. The structure of the network is more complex. Its core structure can be divided into four parts to analyze, including forget gate, input gate, cell state and output gate.

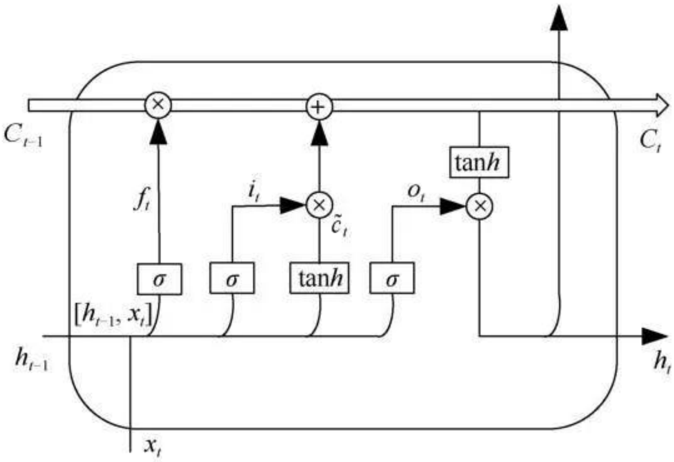

Figure 1. Schematic diagram of long short-term memory neural network/

Splicing the current time step input x_t and the previous time step hidden state h_{t-1} to get $[h_{t-1}, x_t]$. Then transform it through a fully connected layer, and finally activate it through the sigmoid function to get f_t:

$$f_t = \sigma\left(W_f \cdot [h_{t-1}, x_t] + b_f\right) \tag{4}$$

Formula (4) means that how much past information carried by the cell state of the previous layer is forgotten is determined based on the current time step input and the previous time step hidden state h_{t-1}

$$i_t = \sigma(W_i \cdot [h_{t-1}, x_t] + b_i) \tag{5}$$

Formula (5) is almost the same as the forget gate formula, the difference is the object to be acted on that it represents the filtering of input information.

$$\tilde{C}_t = tanh(W_C \cdot [h_{t-1}, x_t] + b_C) \tag{6}$$

Formula (6) is the same as the internal structure calculation of the traditional RNN , and the current cell state is obtained.

$$C_t = f_t \cdot C_{t-1} + i_t \cdot \tilde{C}_t \tag{7}$$

Formula (7) is the cell state update. Multiply the forget gate value just obtained by the C_{t-1} obtained at the previous time step, and then multiply the input gate value by the unupdated $\tilde{C}_t$ obtained at the current time step. The final result is obtained as part of the input for the next time step.

$$o_t = \sigma(W_o \cdot [h_{t-1}, x_t] + b_o) \tag{8}$$

Formula (8) is the gate value of the output gate

$$h_t = tanh(C_t, o_t) \tag{9}$$

Formula (9) is the hidden state h_t generated by the gate value of formula (8), which will act on the updated cell state and substitute into the activation function. The final result is obtained as part of the input for the next time step.

2.2. A Combinatorial Prediction Model Based on Generalized Induced Ordered Weighted Harmonic Mean Operator and Vector Angle Cosine

2.2.1. Constructing Operators

Suppose the observed value of the indicator sequence of a certain socio-economic phenomenon is $\{x_t, t = 1,2,\dots,N\}$, and there are m feasible single-item prediction methods to predict it. x_{it} is the predicted value (or fitting value) of the i-th prediction method at the t time. Let $l_1, l_2, \dots, l_m$ be the weighted coefficients of m single predictions in combined predictions, which satisfy normalization and non-negativity, that is $\sum_{i=1}^{m} l_i = 1,\ l_i \geq 0,\ i = 1,2,\dots,m$.[7]

Constructing the accuracy formula:

$$a_{it} = \begin{cases} 1 - |(x_t - x_{it})/x_t|, & |(x_t - x_{it})/x_t| < 1 \\ 0, & |(x_t - x_{it})/x_t| \geq 1 \end{cases} \tag{10}$$

Among them $i = 1,2,\dots,m$ and $t = 1,2,\dots,N$. Call a_{it} the prediction accuracy of the i-th prediction method at time t. The prediction accuracy is used as the induction value of the prediction value. At this time, the prediction accuracy of m single prediction methods at time t and the prediction value of their corresponding sample interval constitute m two-dimensional arrays $\langle a_{1t}, x_{1t}\rangle, \langle a_{2t}, x_{2t}\rangle, \dots, \langle a_{mt}, x_{mt}\rangle$.

Let $L = (l_1, l_2, \dots, l_m)^T$ be the weighted vector of IOWHA of various prediction methods in the combined prediction. Arrange the prediction accuracies of the m prediction methods at time t in descending order, and let $a - index(it)$ be the subscript of the i-th largest prediction accuracy:[9]

$$\hat{x}_t = F(\langle a_{1t}, x_{1t}\rangle, \langle a_{2t}, x_{2t}\rangle, \dots, \langle a_{mt}, x_{mt}\rangle) = 1 \backslash \sum_{i=1}^{m} \frac{l_i}{x_{a-index(it)}} \tag{11}$$

It is called the combined prediction value of the IOWHA operator. This formula shows that the weight coefficient of the combined prediction has nothing to do with the single prediction method, but is closely related to the prediction accuracy of the single prediction method at each time point.

Let $X = [x_1, x_2, \dots, x_N]^T$, $X_i = [x_{i1}, x_{i2}, \dots, x_{iN}]^T$, $\hat{X} = [\hat{x}_1, \hat{x}_2, \dots, \hat{x}_N]^T$, then X represents the actual value vector of the predicted object, X_i represents the predicted value vector of the i-th prediction method. $\hat{X}$ represents the combined predicted value vector.

2.2.2 Constructing the cosine of the vector angle

$$\eta_i = \frac{\sum_{t=1}^{N} x_t x_{it}}{\sqrt{\sum_{t=1}^{N} {x_t}^2}\sqrt{\sum_{t=1}^{N} {x_{it}}^2}} \tag{12}$$

Among them $i = 1,2,\dots,m$. η_i is called the cosine of the angle between the predicted value vector X_i of the i-th prediction method and the actual value vector X of the prediction object

$$\eta = \frac{\sum_{t=1}^{N} x_t \hat{x}_t}{\sqrt{\sum_{t=1}^{N} {x_t}^2}\sqrt{\sum_{t=1}^{N} \hat{x}^2}} \tag{13}$$

η is called the cosine of the angle between the combined predicted value vector $\hat{X}$ of IOWHA and the actual value vector X of the predicted object.

Let $F_{ij} = \sum_{t=1}^{N} x_{a-index(it)} x_{a-index(jt)}$, $i,j = 1,2,\dots,m$ and $F = \left(F_{ij}\right)_{m\times m}$ be the combined prediction information matrix of the angle cosine of IOWHA. Then we have:

$$\sum_{t=1}^{N} \hat{x}_t^{\,2} |= \sum_{t=1}^{N}\left(\sum_{i=1}^{m} l_i x_{a-index(it)}\right)^2$$
$$| = \sum_{i=1}^{m}\sum_{j=1}^{m} l_i l_j \left(\sum_{t=1}^{N} x_{a-index(it)} x_{a-index(jt)}\right) \quad (14)$$
$$= \sum_{i=1}^{m}\sum_{j=1}^{m} l_i l_j F_{ij} = L^T FL$$

$$\eta = \frac{\sum_{i=1}^{m} l_i \sum_{t=1}^{N} x_t x_{a-index(it)}}{\sqrt{\sum_{t=1}^{N} x_t^{2}}\sqrt{L^T FL}} \quad (15)$$

It is recorded as $\eta(l_1, l_2, \ldots, l_m)$. The larger the value of formula (15) is, the more effective the combination prediction method is.

$$max\,\eta\,(l_1, l_2, \ldots, l_m) = \frac{\sum_{i=1}^{m} l_i \sum_{t=1}^{N} x_t x_{a-index(it)}}{\sqrt{\sum_{t=1}^{N} x_t^{2}}\sqrt{L^T FL}} \quad (16)$$

$$s.t\begin{cases} \sum_{i=1}^{m} l_i = 1, \\ l_i \geq 0, i = 1,2, \ldots, m \end{cases} \quad (17)$$

3. DATA DESCRIPTION AND MODEL EMPIRICAL STUDY

3.1. Variable Selection

From the perspective of carbon price fluctuation characteristics and influencing factors, compared with the other four pilots, Guangzhou's carbon emission trading market is more developed, and there is a positive correlation between yield and risk. Considering this aspect, the carbon emission price of Guangzhou's carbon trading market is taken as the research object of this article. The sample period is from January 2015 to March 2023, and the data frequency is monthly. The average transaction price of Guangdong's carbon emission right price is shown in the figure 2:

Figure 2. Average transaction price of carbon emission quota in Guangdong

At present, Chinese carbon emission quota allocation is mainly free allocation, so the impact of the supply of carbon emission quotas on prices is not considered. Only the factors affecting carbon price changes are considered from the demand level. This paper mainly selects variables from four dimensions: energy prices, macroeconomics, financial markets and ecological environment.

3.1.1 Energy Prices

Carbon-containing products such as fossil energy are an important driving force for the development of the energy industry and one of the main driving forces for the development of modern industry. At present, energy can be divided into two categories, one is traditional energy and the other is clean energy [3]. They have different transmission mechanisms for the price of carbon emission right. Take traditional energy represented by coal as an example to explain the transmission mechanism: when the price of coal rises, the cost of using coal for emission reduction enterprises increases, and enterprises will tend to choose clean energy to replace coal. At this time, the carbon emissions of enterprises decrease, the supply of carbon emission rights market increases, and the price of carbon emission rights will fall; conversely, when the price of coal falls, the price of carbon emission rights will rise. The transmission mechanism of clean energy represented by natural gas: when the price of natural gas falls, emission reduction enterprises will consider increasing the use of natural gas to reduce carbon emissions. At this time, the supply of carbon emission rights market increases and the price of carbon emission rights falls; conversely, when the price of natural gas rises, the price of carbon emission rights rises. The main energy sources in the current society include coal, natural gas and oil. Generally, under the same production conditions, the use of coal produces the most carbon emissions, followed by oil, and the least is natural gas. The price changes of these three energy sources will affect the energy choices of emission reduction enterprises, so the relative price fluctuations between the three will cause fluctuations in the price of carbon emission rights [14].

3.1.2 Macroeconomics

The development of the macro economy will affect the price of carbon emission rights to a certain extent. This is mainly reflected in the fact that when the macro economy is in good condition, carbon-intensive industries such as industry and transportation are developing well, and enterprises will expand their production scale. At this time, the carbon emissions of society will increase, the demand for carbon emission rights market will increase, and the price of carbon emission rights will rise. When the macro economy is in poor condition, carbon-intensive enterprises such as industry and transportation lack the motivation to develop. At this time, the scale of production will be reduced, the carbon emissions of society will decrease, the supply of carbon emission market will increase, and the price of carbon emission rights will fall.

3.1.3 Financial Markets

Whether the financial market is prosperous or not is one of the factors that affect the price of carbon emission rights. Specifically, when the financial market is prosperous, the economy develops rapidly, the society has full confidence in the financial market, consumer demand increases, the scale of production expands, and the social carbon emissions increase. At this time, the price of carbon emission rights rises; on the contrary, when the financial market is sluggish, the economic development speed is slow, the public confidence declines, consumer demand decreases, the scale of production shrinks, and the social carbon emissions decrease. At this time, the price of carbon emission rights decreases.

3.1.4 Ecological environment

AQI is an observation index for determining a city's air quality. The smaller the value of this index, the better the air quality. To a certain extent, it represents the quality of air quality. When the AQI index is higher, it means that the emission reduction enterprises produce more carbon emissions in the production process. In order to achieve the emission reduction target, the demand for carbon emission rights of emission reduction enterprises increases, and then the carbon emission price increases.

Based on the influencing factors that have been studied: energy prices, macroeconomics, financial markets and ecological environment. The following variables are selected:

Table 1. Selection of influencing factors variables

Influencing factors	variable name	Variable alias
Energy Prices	Jingtang Port: Closing price: Thermal coal (Q5500)	JG
	Guangzhou Port: warehouse price: Indonesian coal (Q5500)	GG
	Futures settlement price: WTI	WTI
	OPEC: Crude Oil Basket Price	OPEC
	Liquefied Natural Gas LNG: Nationwide	LNG
Macroeconomics	Guangdong: PPI	GPPI
	PPI: Petroleum, coal and other fuel processing industry	PPI
	PMI Index	PMI
	Production PMI Index	PPMI
	PMI: Purchase price of major raw materials	MPMI
Financial market	Guangzhou carbon emission quota trading volume	GCEA
	Average exchange rate: USD to RMB	USDCNY
	Shanghai Composite Index	SCI
	CSI 300 Index	CSI300
	CSI 500 Index	CSI500
	Industrial value added	EVA
ecosystem	Air Quality Index (AQI): Guangzhou	AQI

3.2. Data Processing

First, the missing values in the sample data are filled with variable averages; secondly, based on the 3σ outlier identification method, that is, assuming that the data obeys a normal distribution, the probability of $\pm 3\sigma$ is 99.7%. Therefore, the probability of occurrence of values other than 3σ from the average value is $P(|x-\mu| \cdot 3\sigma) = 0.003$, which is a very small probability event and should eliminate them and replace them with the average of the variables [15]. Finally, the range standard method is used to dimensionless process the original variable data to reduce the dimensional difference between variables and truly reflect the dependence between the explanatory variables and the explained variables [8].

To facilitate modeling and validation, the data is divided into two parts, where the training sample includes the first 90% of the observations of all sequences, and the rest are used as test samples. Four prediction error evaluation indicators are used: root mean square error (RMSE), mean absolute error (MAE), mean absolute percentage error (MAPE) and mean square percentage error (MSPE).

$$RMSE = \sqrt{\frac{1}{N}\sum_{i=1}^{N}(x_i - \hat{x}_i)^2} \tag{18}$$

$$MAE = \frac{1}{N}\sum_{i=1}^{N}|x_i - \hat{x}_i| \tag{19}$$

$$MAPE = \frac{1}{N}\sum_{i=1}^{N}\frac{|x_i - \hat{x}_i|}{x_i} \tag{20}$$

$$MSPE = \sqrt{\frac{1}{N}\sum_{i=1}^{N}\left[\frac{(x_i - \hat{x}_i)}{x_i}\right]^2} \tag{21}$$

3.3. Sub-model Prediction Results

3.3.1. Ridge Regression

First, the variables were regressed using the least squares method. The results showed that the VIF (collinearity) of the independent variable was too large, so ridge regression was considered for multiple regression. Since the application object of this model is time series, the data lagged by one period of the dependent variable, that is The average transaction price of Guangdong carbon emission allowances in the last period (GCEA-1) were added for ridge regression analysis. The final results of the variables selected by the t-test are as follows:

Table 2. Ridge regression model results

K=0.151	B	t	P	R^2	Adjusting R^2	F
constant	0.069	3.551	0.001***	0.944	0.941	307.574 (0.000***)
GCEA	0.09	8.045	0.000***			
SCI300	0.07	5.747	0.000***			
PPMI	-0.103	-3.656	0.000***			
GCEA(-1)	0.604	19.045	0.000***			

Note: ***, **, and * represent 1%, 5%, and 10% significance levels, respectively.

From table 2, we can see that use the variance expansion factor method to find the K value of 0.151. It can be seen that under this sub-model method, the variables GCEA, SCI300, PPMI and GCEA(-1) have a significant impact on the current period transaction average price, among which the impact coefficient of GCEA(-1) is 0.604, and the PPMI index has a negative impact on the current period transaction average price, with an impact coefficient of -0.103.

3.3.2. Random Forest Regression

In order to avoid the problem of overfitting on the training set due to unreasonable division of the data set, this article adopts three-fold cross-validation. The data set is divided into three mutually exclusive subsets of similar size. Each time, the union of the two subsets is used as the training set, and the remaining one is used as the test set. Training and testing are performed three times. The following settings are made for this submodel: the minimum number of samples for internal node splitting is 2, the minimum number of samples for leaf nodes is 1, the maximum depth of the tree is 10, the maximum number of leaf nodes is 50, and the number of decision trees is 100. Perform sampling with replacement.

Table 3. Importance of random forest feature variables

Feature Name	GCEA	WTI	OPEC	JG	PPI	CSI300
Importance	68.40%	10.30%	7.90%	5.00%	4.50%	3.90%

The feature importance was calculated by establishing a random forest, and finally 6 important variable data were obtained. Among them, the feature importance of Guangzhou carbon emission quota trading volume (GCEA) was the highest, at 68.4%, and the feature importance of the CSI 300 Index was the lowest, at 3.9%.

3.3.3. Long Short-Term Memory neural network

For this experiment, the hardware configuration of the experimental environment is a laptop with Intel(R) Core(TM) i5-8265U CPU @ 1.60GHz and NVIDIA GeForce MX150. The project development environment is IDE: PyCharm, Python3.8, PyTorch1.13.0, and the device is GPU. The optimizer adopted is Adam (Adaptive Moment Estimation), the model hidden layer is set to 2. The learning rate is 0.002 and the maximum number of training times is 100. The sequence length is set to 6, and the 6 vectors are taken in a loop to predict the result of the 7th vector.

Random forest feature importance selection was performed for all variables. Through each node in the decision tree that is conditional on a feature, calculate how much each feature reduces the impurity of the tree. The average reduced impurity of the decision tree forest is thus calculated, and this is used as the value for feature selection. Finally, GCEA, WTI, GPPI, PPI, USCCNY, MPMI, CSI500 are selected as input items. Figure 3 shows the fitting of the long short-term memory structure neural network training set, and the fitting results are good.

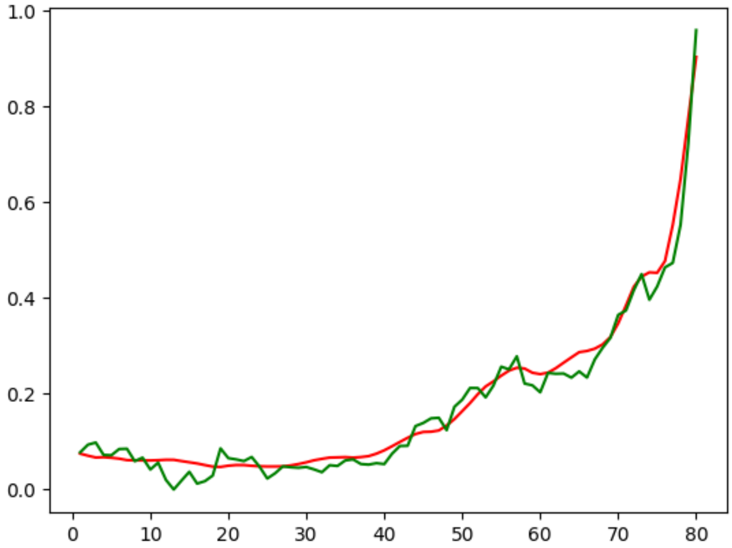

Figure 3. Fitting effect of LSTM training set

3.3.4. Sub-model prediction results

Table 4. Prediction results of sub-models

time	Actual value x_t	Ridge regression predictions x_{1t}	Random Forest Regression Prediction x_{2t}	LSTM prediction x_{3t}
1	0.935	0.680	0.778	1.054
2	0.958	0.711	0.893	1.054
3	0.958	0.721	0.878	1.070
4	0.933	0.703	0.819	1.056
5	0.923	0.697	0.793	1.027
6	0.931	0.707	0.807	0.954
7	0.914	0.744	0.726	0.883
8	0.901	0.694	0.733	0.799
9	0.922	0.630	0.730	0.758
10	1.000	0.659	0.625	0.719

Table 5. Sub-model prediction errors

error	RMSE	MAE	MAPE	MSPE
Ridge Regression	0.247	0.243	0.258	0.068
Random Forest Regression	0.227	0.218	0.232	0.058
LSTM	0.131	0.114	0.121	0.043

From the table 5, we can see that the four error indicators of the LSTM are the smallest compared to other methods, and this method has the best prediction effect. However, the error indicator of the ridge regression prediction value is the largest, and the performance is the worst.

3.4. Combined Prediction Results

The prediction accuracy of each sub-model is calculated according to the prediction accuracy formula:

Table 6. Prediction accuracy of sub-model

time	Ridge regression prediction accuracy	Random Forest Regression Prediction Accuracy	Prediction accuracy of LSTM
1	0.728	0.832	0.873
2	0.742	0.932	0.900
3	0.753	0.917	0.884
4	0.753	0.878	0.868
5	0.755	0.860	0.887
6	0.760	0.867	0.975
7	0.814	0.795	0.967
8	0.771	0.814	0.887
9	0.683	0.791	0.822
10	0.659	0.719	0.734

The combined prediction value of the IOWHA operator is calculated according to formula (16). The optimal weight coefficient of the combined prediction model based on IOWHA and vector angle cosine is calculated using the MATLAB optimization toolbox:

$$l_1 = 0.996377196,\ l_2 = 0.003162239, l_3 = 0.000460565$$

Table 7. Comparison of combined prediction results

time	Actual value	Ridge regression predictions value	Random Forest Regression Prediction value	LSTM prediction value	Combined prediction value
1	0.935	0.680	0.778	1.054	1.053
2	0.958	0.711	0.893	1.054	0.893
3	0.958	0.721	0.878	1.070	0.879
4	0.933	0.703	0.819	1.056	0.820
5	0.923	0.697	0.793	1.027	1.026
6	0.931	0.707	0.807	0.954	0.953
7	0.914	0.744	0.726	0.883	0.882
8	0.901	0.694	0.733	0.799	0.798
9	0.922	0.630	0.730	0.758	0.757
10	1.000	0.659	0.719	0.734	0.734

Table 8. Comparison of combined prediction errors

error	RMSE	MAE	MAPE	MSPE
Ridge Regression	0.780	0.243	0.258	0.083
Random Forest Regression	0.719	0.218	0.232	0.076
LSTM	0.131	0.114	0.121	0.043
Combined prediction value	0.126	0.107	0.113	0.041

From the table 8, we can see that the combined prediction value is smaller than ridge regression, random forest regression and LSTM in terms of root mean square error (RMSE), mean absolute error (MAE), mean absolute percentage error (MAPE) and mean square percentage error (MSPE) . Therefore, based on the theorem of superior combination prediction of combined prediction model, that is $\eta(l_1, l_2, l_3) \geq \eta_{max}$, the optimal combination prediction model based on generalized induced ordered weighted harmonic mean operator and vector angle cosine is called superior combination prediction.

4. CONCLUSION

The Chinese carbon emission market is currently in a phase of development and enhancement. Carbon emission prices play a crucial role in this market as they serve as a key indicator of its performance. Enhancing the accuracy of carbon emission price prediction models at a theoretical level can provide valuable insights into the market's operational status, the formation of reasonable carbon emission prices, and the efficient allocation of carbon emission rights. This, in turn, can enable the government to implement more effective measures for reducing carbon emissions, drive the advancement of the Chinese low-carbon economy at the financial market level, and facilitate the achievement of the "Dual Carbon Target ".

This study proposes a novel approach for predicting the transaction price of carbon emission quotas in the Chinese carbon emission market using a combination of deep learning and traditional prediction methods. By integrating deep learning techniques with multivariate regression methods and leveraging the combined prediction of the IOWHA operator and vector angle cosine, with varying weights assigned to different feature sub-models, the proposed approach mitigates the limitations of individual sub-models while capitalizing on their strengths to enhance prediction accuracy. The combined prediction strategy presented in this study represents an optimal amalgamation of techniques.

Future research endeavors will focus on exploring the interplay between the carbon emission market and other markets, employing diverse feature variable selection methodologies to identify effective influencing factors, and integrating particle algorithms to transform the weight analysis in the combined prediction model from a static to a dynamic framework. These advancements hold the potential to further boost prediction accuracy and contribute to the ongoing refinement and evolution of carbon emission market forecasting techniques.

REFERENCES

[1] Guo, L.J. and Z, J.H. (2022). Wheat yield prediction based on IOWA operator combined with grey neural network. *Grain and Oils*, 35(10): 26-30.

[2] Wang, Z.H. and Hu, Y. (2019). Calculation of price distortion degree of China's carbon emission trading market based on shadow price model. *Ecological economy*, 35(05): 13-20.

[3] Zhou, H. and Z, Y.F. (2021). Research on an improved crude oil price combination forecasting optimization strategy. *Systems Engineering - Theory & Practice*, 41(10): 2660-2668.

[4] Yi, L., Yang, L., Li, C.P. (2017). Research on the influencing factors of EU carbon price and its enlightenment to China. *Chinese Population, Resources and Environment*, 27(06):42-48.)

[5] Zou, Y.S. and Wei, W. (2013). Research on the influencing factors of spot price of carbon emission certified emission reduction (CER). *Journal of Financial Research*, 10: 142-153.

[6] Wang, Q. and Lu, J.J. (2018). Regional heterogeneity of the impact of short-term interest rate fluctuations on carbon trading prices. *Social Sciences Series*, 1: 101-110.

[7] Yuan, H.J. and Yang, G.Y. (2010). A superior combination prediction model based on IOWA operator of closeness. *Statistics and Information Forum*, 25(02): 32-37.

[8] Gao, X.H and Li, X.Q. (2022). Comparison of dimensionless methods in multivariate linear regression models. *Theoretical Discussion*, 38(06): 5-9.

[9] Yuan, H.J. and Hu, L.Y. (2014). Variable weight coefficient interval type combined prediction model of IOWHA operator of vector angle cosine. *Journal of Heze University*, 36(05): 1-7.

[10] Zhao, L.D. (2019). Research on Carbon Trading Price Forecasting——Taking Shenzhen as an Example. *Economic Theory and Practice*, 2: 76-79.

[11] Gong, W.F. and Wang, L.P. (2022). Research on the characteristics of price fluctuations in China's carbon emission rights market: An empirical analysis of five carbon trading pilot projects. *Theory. Methods and Cases*, 2022, 4: 149-160.

[12] Lu, J.Y. (2021). Parameter sensitivity analysis of factors affecting China’s carbon emission rights price. *Soft Science*, 35(05): 123-130.

[13] Lu, J.Y. (2019). Research on the decomposition of factors affecting China's carbon emission rights price based on GA-RS. *Ecological Economy*, 35(11): 42-47+130.

[14] Wei, Q. (2018). Research on the impact of fossil energy price changes on China's carbon trading prices. *Economic Theory and Practice*, 11: 42-45.

[15] Wang, X.Y. (2022). Analysis of influencing factors of carbon emission rights price based on graph structure adaptive Lasso. *Statistics and Information Forum*, 37(04): 73-83.

[16] Zhou, C.B. (2020). Does the carbon emissions trading pilot policy promote China's low-carbon economic transformation? —— An empirical study based on the double difference model. *Soft Science*, 34(10): 36-42+55.

[17] Ji, Q.H. (2018). Research on carbon quota price prediction model based on multivariate linear regression. *Modern Chemical Industry*, 38(04): 220-224.